Chemistry Research Journal, 2017, 2(5):176-185

Available online www.chemrj.org

Research Article

ISSN: 2455-8990
CODEN(USA): CRJHA5

CFD Modeling for Syngas Production from Natural Gas Using Steam Reforming in Nanocatalyst Microreactors

Pouyan Shams Farahsary[1]*, Mehran Moazeni Targhi[1], Farhad Khorasheh[2]

[1]Department of Chemical Engineering, Faculty of Engineering, Islamic Azad University-South Tehran Branch, Tehran, Iran
[2]Department of Chemical Engineering, Faculty of Engineering, Sharif University of Technology, Tehran, Iran

Abstract Production of syngas as a raw and intermediate material is very important for industries. Despite numerous attempts made in industry, there are still many challenges in its production. One of these challenges is effect of temperature on catalyst deactivation and conversion which has a direct effect on yield of process. Thus, this study tends to simulate methane steam reforming process in monolith micro-reactors and evaluate effect of temperature on reactor performance. The values obtained were evaluated by results of experiments and simulations conducted and the model was confirmed. Then, effect of temperature was examined on yield. This study first modelled tubular reactor synthetically. Then, values were validated by results of other studies. Finally, energy, mass and momentum equations as well as the reaction was incorporated in the model. Geometry used in this process was one of the models for monolith reactors used in Knox process in industry. This geometry included a multi-channel porous wall monolith reactor in which reactions occurred within the wall. As the results showed, porous wall monolith reactor allowed 70% conversion. Coke formation which deactivates catalyst can be avoided by keeping temperature over 800 ºC. Thus, this study tended to keep constant temperature (800 ºC) by applying external heat through temperature thermal jacket.

Keywords Syngas, Reforming, Monolith Micro-Reactor, Porous Wall

1. Introduction

Based on input feed used, syngas production can be classified into two different processes, one based on natural gas by hydrocarbons and the other based on coal. If natural gas and heavy hydrocarbons are used as main feed in syngas production, lower investment than coal is needed. Although huge reserves of coal are available at a price cheaper than hydrocarbon resources, economic investment in coal-based syngas production costs triple the cost of units based on natural gas. Due to decreasing oil resources, natural gas seems very suitable for syngas production. Therefore, a cost-effective raw material for syngas production is usually natural gas producing excessive hydrogen-rich gas (steam process), which must be consistent with stoichiometric ratio of syngas. Therefore, syngas production units require a H_2/CO refinery unit or H/CO_2 reverse conversion unit [1]. In general, this study tends to simulate syngas production process from natural gas through methane steam reforming in monolith micro-reactors.

In terms of catalyst, the goal is to help design catalyst, evaluate performance and effect of geometry. Proper channel to display is temperature and concentration profiles in the reactor, assuming that all channels show the same behavior and have no effect on each other. Modeling of complete reactor is the most detailed modeling which

indicates effect of temperature or concentration of different layers on performance of each other; this can be used for evaluation and optimization. As shown in [2] that one-dimensional modelling is applicable for performance of kinetic parameters and effect of variation in variables on performance. In the first model, reactor is considered as a plug; kinetics studies are based on values of empirical studies and resources are considered to evaluate conversion, temperature, pressure and selectivity profiles [3]. In the second modeling, reactor is depicted fully in three dimensions and mass transfer, heat and momentum equations are incorporated in the model. This study tends to evaluate effect of boundary conditions and temperature distribution on performance of reactor and its optimization.
The problem is solved assuming:

- The flow within the reactor is considered laminar at steady state based on ideal gas law;
- Chemical reaction considered in this model only occurs in the walls;
- Mass transfer only occurs within porous channels;
- Heat distribution occurs between channels;
- The flow within channels is layered and Brinkman equation is used for porous areas;
- Since 75% of the compound is steam, fluid is diluted in simulation and steam properties are considered for the flow within the channel.

2. Modeling and methods

2.1. Governing Equations and Boundary Conditions

First, tubular reactor process is considered at steady state.

$$\frac{dF_i}{dV} = R_i \quad (1)$$

Where, F_i is flow rate for each component, V represents volume of channel or reactor and R_i is velocity of reactions for the component i. Energy balance for ideal gas is written as:

$$\sum F_i \, C_{p,i} \frac{dT}{dV} = w + Q + Q_{ext} \quad (2)$$

Where, $C_{p,i}$is specific heat capacity of components, Q_{ext} is external heat added per unit volume to the system (Q_{ext} =0 in adiabatic mode), W_s is external work imposed on the system (W_s=0).
In above equation, Q represents heat produced by the reaction, which is calculated by equation (3) where H_i represents temperature and r_i represents velocity of reaction.

$$Q = \sum_j H_j \, r_j \quad (3)$$

In three-dimensional modelling mass, momentum and heat balances are considered. Temperature and concentration profiles are shown for the reactor. Since no mass transfer occurs between channels, mass transfer is considered one dimensional in each channel. Considering the type of walls in the reactor, heat transfer is considered three dimensional; this heat transferred between channels and walls by conductance mechanism.

2.2. Mass Transfer

Mass transfer occurs with two diffusion and displacement mechanisms. In diffusion mechanism, reactants enter the porous walls, where they react under catalyst and the product moves in main flow through porous section. Displacement mechanism occurs along the channel. No mass transfer occurs between channels. COMSOL multi-physics [4] has installed a specific physic called as species transport in porous media which includes a fixed porous part and a moving fluid part. Given similarity of the considered physic and reactor conditions, this physic is used for mass transfer.

$$\nabla.(-D_i \nabla c_i) + u.\nabla c_i = R_i \quad (4)$$

$$N_i = -D_i \nabla c_i + u c_i \quad (5)$$

where, D_i represents diffusion rate, R_i represents reaction, C_i is concentration of the component i and u is velocity.Boundary conditions are listed in Table 1.

Table 1: Boundary conditions of mass transfer equations

Baseline values	Concentration in the first model
Input flow	$C_i = C_{0,i}$
Output flow	$-nD_i\nabla c_i = 0$
Reaction	Values obtained from the first model

2.3. Momentum

The average path traveled in atmospheric pressure is 10^{-9} and system size is 10^{-3}; thus, Knudsen number is less than 0.01. Therefore, distribution of gas flow within the channel can be described by using Navier-Stokes and continuity equations.

$$\rho(u.\nabla)u = \nabla.[-pI + \mu(\nabla u + (\nabla u)^T)] + F \quad (6)$$

Nabla∇ represents the first order derivative, ρ represents the density calculated using ideal gas, μ is gas mixture viscosity calculated by Wilke method, u is velocity vector, p is pressure and T represents matrix transpose.

Navier-Stokes equations are not valid in porous solid area; thus, Brinkman equations are used. Table 2shows boundary conditions in dynamic of Navier-Stokes equations.

$$\frac{\rho}{\varepsilon_p}(u.\nabla)\frac{u}{\varepsilon_p} = \nabla.\left[-pI + \mu\frac{\mu}{\varepsilon_p}(\nabla u + (\nabla u)^T) - \frac{2\mu}{3\varepsilon_p}(\nabla.u)l\right] - \left(\mu k^{-1} + \beta_F|u| + \frac{Q_{br}}{{\varepsilon_p}^2}\right)u + F \quad (7)$$

ε_p represents porosity and Q_{br} represents diffusion in porous component. Darcy term should also be considered.

Table 3: Boundary conditions in dynamic of Navier-Stokes equations

Item	Description
External wall	$u = 0$ (Non-slippery)
Input	$u_z = u_0$ (Uniform velocity profile)
Output	$P = P_0$ (Room pressure)
Initial	$u_z = u_0, P = P_0$

2.4. Heat Transfer

Heat transfer occurs in reactor in two forms. The first form occurs through fluid along the channel and porous structure by displacement and conductance mechanism. Heat transfer equation for fluid and porous are is written as:

$$\rho C_p u.\nabla T = \nabla.(k\nabla T) + Q + Q_{vh} + W_p \quad (8)$$

Where, the first term is reduced and simplified due to steady conditions. Considering z-axis transfer, the equation can be simplified as follows.

Here, C_p is heat capacity of the gas, k is constant thermal conductivity of gas and solid and Q is heat produced by chemical reactions. Thermal conductivity ranges from 0.8 to 5 for ceramic monoliths [5], 25 for metal monoliths and 0.02 to 0.005 for gases. Porosity is set at 0.8 for porous monolith walls. In the second form of heat transfer, flow is in the form of conductance through protective walls radially. Boundary conditions are listed in Table 3.

Table 4: Boundary conditions of heat equation

Baseline values	Values obtained from the first model
Heat source	Values obtained from the first model
Temperature	$T = T_0$
Output Current	$-n.(-k\nabla T) = 0$
Thermal flux	$-n.(-k\nabla T) = q_0$

2.5. Kinetics

Thermodynamic data needed for energy equations are based on Chemkin and NASA format. Polynomial terms representing thermodynamic properties are as follows.

$$C_{p_i} = R(a_1 + a_2T + a_3T^2 + a_4T^3 + a_5T^4) \quad (9)$$

$$H_i = R(a_1T + a_2T^2 + a_3T^3 + a_4T^4 + a_5T^5) \quad (10)$$

$$S_i = R\left(a_1 lnT + a_2T + \frac{a_3}{2}T^2 + \frac{a_4}{3}T^3 + \frac{a_5}{4}T^4 + \frac{a_6}{5}T^5 + a_7\right) \quad (11)$$

WhereC_p denotes heat capacity, T is temperature, and R is general constant of gases. Moreover, hi represents molar enthalpy and Si represents molar entropy; α1 to α5 are heat capacity, α6 is formation enthalpy at 0 K and α_7 is formation entropy at 0 K. Numerical coefficients provided by NASA are presented for temperatures above 1000 K and lower. Real enthalpy is calculated by:

$$H(T) = \Delta Hf(298) + [H(T) - H(298)] \quad (12)$$

2.6. Catalysts

The key element in design of a reforming process is to find an optimal setup for catalytic-system. So many parameters should be considered in this selection to provide desired conversion and selectivity. According to [6] Ni-based supported Al_2O_3/AL_2O_4 catalysts shows good results in terms of performance and costs in reforming process as well as noble metals (Pt, Rh).

2.7. Geometry

Due to high volume of calculations in the three-dimensional model and hardware limitations, simulation was done on one-eighth of the real model (45 degrees) as shown in Figure 1. Symmetry planes are considered on both sides of the model. Different zones and boundary conditions are considered in modelling as follows [7].

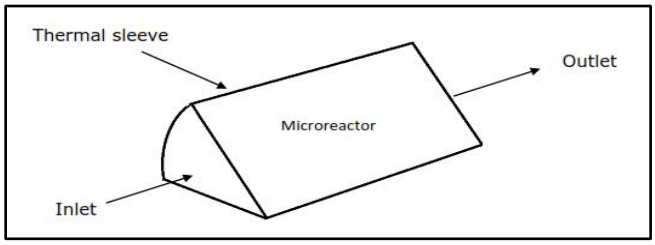

Figure 1: Schematic model

Zones: walls and channels

Boundary parts: inlet, outlet, symmetry, inlet walls, outlet walls, monolith surface

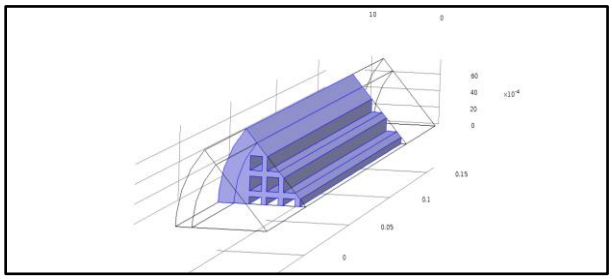

Figure 2: Geometry of monolith reactor with porous walls

2.8. Meshing

To solve the problem, geometry is meshed to elements with small dimensions. To mesh this system, inlet surface of the reactor is meshed by free square elements which include 120 boundary elements and 109 elements in edges.

Then, these meshes are distributed along the reactor to 50 elements which totally includes 6000 elements. Meshes are very fine in inlet and walls to solve concentration gradient more accurately.

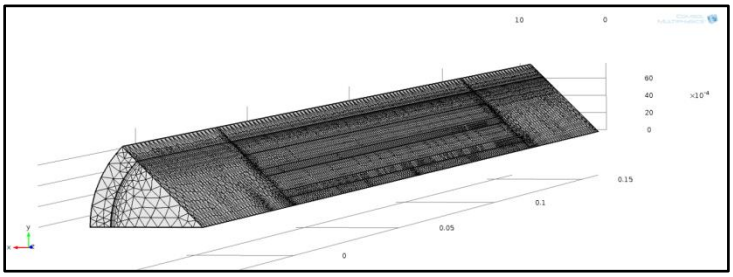

Figure 3: Schematic meshing of monolith reactor

3. Results

In the first modelling, reactor is considered in the form of plug. Figure 4 shows methane conversion at different input temperatures. At 800℃, conversion rate is 68%, which can increase to 100% at 1000℃. In the main model, this value can increase by changing parameters such as temperature, heat flux and input molar flow.

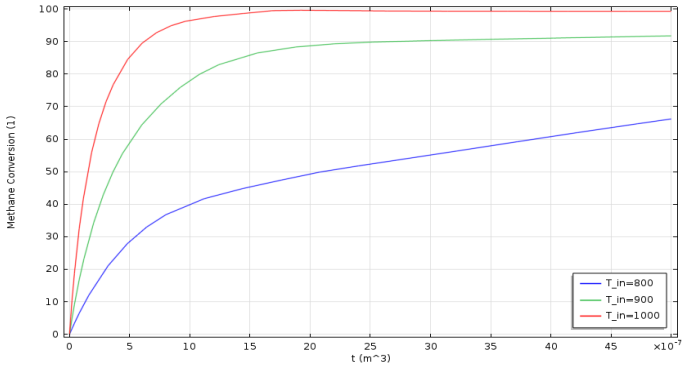

Figure 4: Methane conversion rate along the reactor at different temperatures

Figure 5 shows selectivity of hydrogen production at different temperatures. Obviously, selectivity does not exceed 0.8 at 1000℃. Table 4 calculates error of values obtained in simulation and experimental values obtained by Irani et al (2011).

$$Yield\ H_2 = \left(\frac{F_{H_2 outlet}}{2 \times F_{CH_4 inlet} + F_{H_2 outlet}}\right) \times 100 \qquad (13)$$

Table 5: Comparison of selectivity in the simulated model and experimental value

Temperature	Simulated Model	Experimental Values	Error
800℃	68	79.1	4

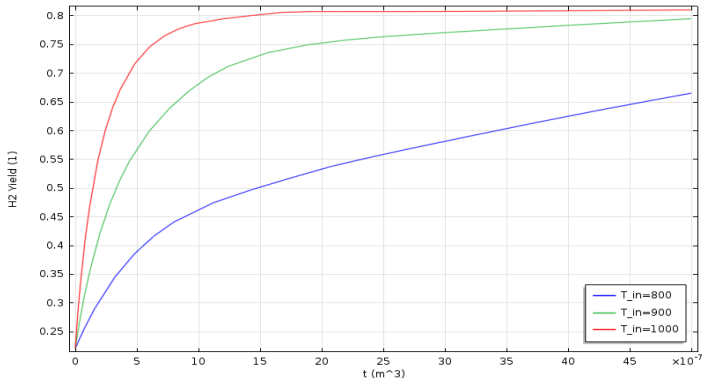

Figure 5: Yield of hydrogen produced at different temperatures

Figure 6 depicts flow rate of components versus unit volume of reactor and its general trend.

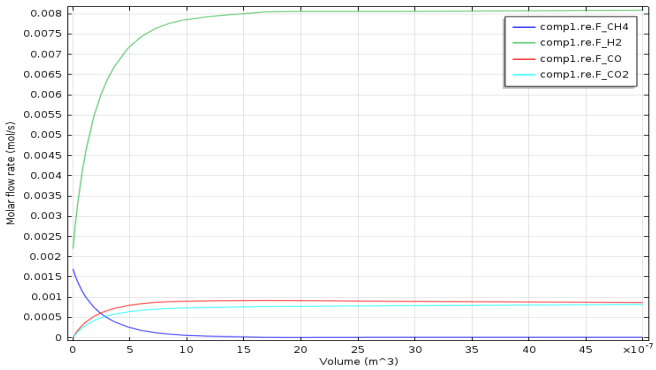

Figure 6: Molar flow rate versus volume

3.1. Solution Independence of Meshing Grid

To evaluate solution independence of meshing grid, average velocity is calculated in coarse, medium and fine meshing. Table 5 shows these three types of meshing.

Table 6: Comparison of meshes

Meshing	N	Minimum and maximum	Average velocity
Coarse	102153	0.014	0.001
Medium	176232	0.03847	0.00103
Fine	402517	0.024	0.00117

Since difference in average velocity is less than 0.05 between medium and fine meshing, it is logical to use normal meshing due to lower runtime.

3.2. Problem Validation

Results of simulation are relatively consistent with values obtained from Vincenzo Palma et al [3]. Margin of error between simulation and experimental values results from error in numerical calculations and reaction conditions.

Maximum error is 17%, which is acceptable considering computational error and modelling error and conditions. Figure 7 and 8 compare values obtained from simulation and real values resulting from experiments.

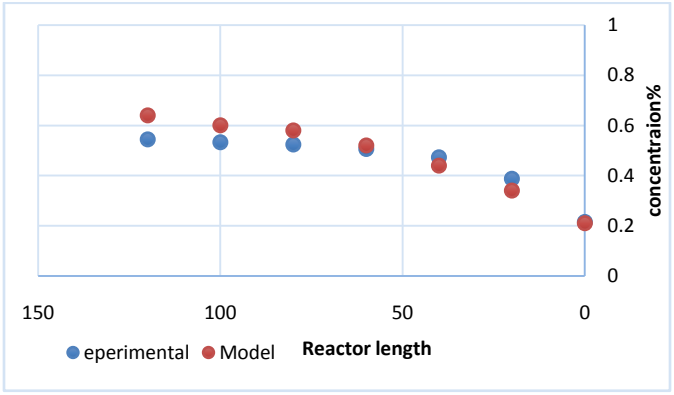

Figure 7: Comparison of hydrogen concentration profile at 800 ℃

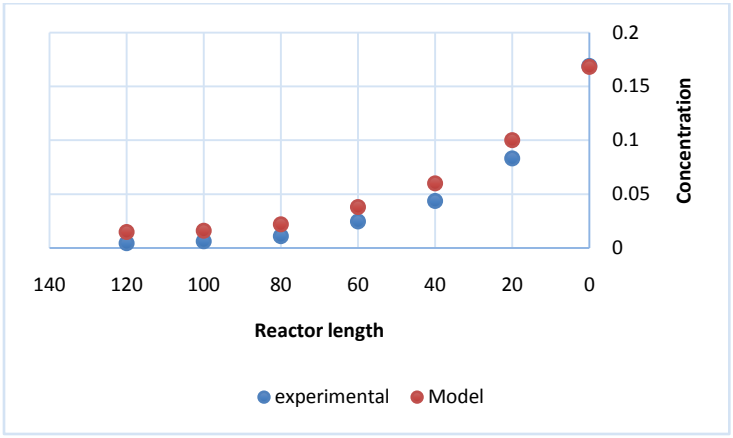

Figure 8: Comparison of methane concentration profile at 800 ℃

3.3. Effect of Initial Temperature on Reactor Yield

To evaluate effect of initial temperature, GHSV is set at 5000 and 4000 h^{-1}, respectively; then, yield is calculated at 700, 800 and 900℃. The results are shown in Table 6. According to results, yield concentration reaches equilibrium at temperatures over 800℃. The results obtained from simulation are consistent with experimental values. According to Table 6, the difference in conversion rate is less than 1.1% between two temperatures; this can be attributed to structure of reactor which prevents full temperature distribution along the reactor. Considering cost of temperature production and negative effects of increasing temperature on the system, 800℃ is suitable for this process.

Table 7: Methane conversion rate to inlet temperature

	T(℃)	Methane conversion %
GHSV=5000	700	66.4
Q=4000	800	69.6
	900	70.7

3.4. Effect of Flow Rate

This section evaluates effect of flow rate on conversion rate in the reaction by variations in Gas Hourly Space Velocity (GHSV). GHSV is calculated based on volumetric flow rate on catalyst volume (as an inhibitor).

$$GHSV = \frac{Q_{tot}\left[\frac{m^3}{h}\right]}{V_{cat}\,[m^3]} \qquad (14)$$

GHSV varies from 250 to 25000. Here, it occurs on 250, 5000, 10000, 20000 and 30000. According to Table 7, increase in GHSV to 30000 reduces methane conversion rate. This can be attributed to lower retention time for reaction in monoliths. However, the increase in this reduction reduces temperature significantly; this prevents decomposition reaction of methane and carbonization causing catalytic poisoning. According to the studies conducted, temperature drop less than 650℃ significantly increases carbonization and consequently carbon poisoning. Therefore, optimal GHSV is 5000.

Table 7: Variations in methane and hydrogen by variations in GHSV

	GHSV [h^{-1}]	CH_4 concentration, dbvol%	H_2 concentration, dbvol%
Q=4000, T=800	250	009118	0.85937
	5000	0.15995	0.63124
	10000	0.18041	0.60217
	20000	0.28785	0.48937

30000	0.33.009	0.44798

Values shown in Table 7 are average volumetric concentration in the reactor. Figure 9 compares values obtained in simulation and experimental values, which indicates good consistency.

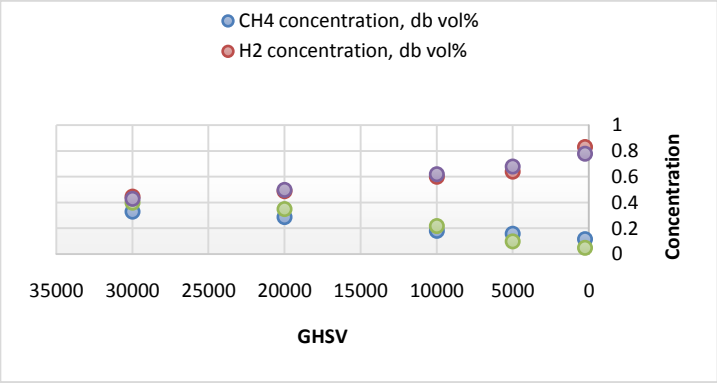

Figure 9: Comparison of methane and hydrogen values in different GHSVs and experimental values

3.5. Effect of Heat Flux on Yield

Since the reaction is endothermic, adiabatic nature of the process considerably reduces temperature and conversion rate. By causing heat flux through thermal jacket in reactor wall, therefore, temperature changes can be controlled, temperature drop can be reduced and yield can be increased.

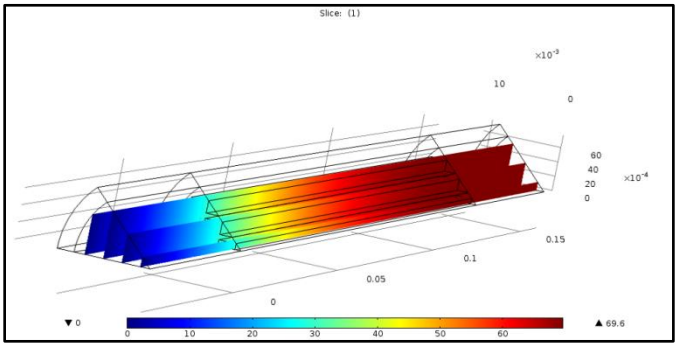

Figure 10: Concentration profile at 4000 thermal flux

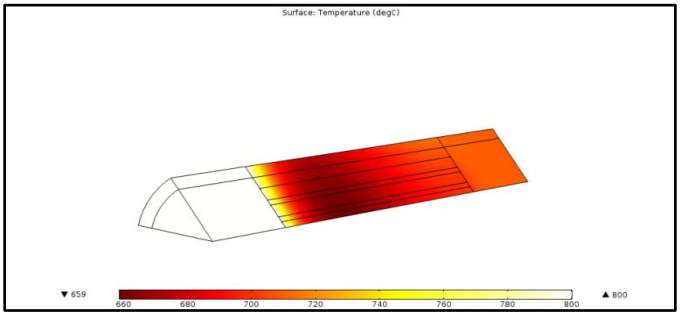

Figure 11: Temperature profile at GHSV=5000 and flux=4000 [mW/cm^2]

As shown in Figures 10 and 11, temperature considerably dropped initially. The first part of the reactor in which reaction does not occur is solely for mixing. With arrival of highly porous part and endothermic reactions, temperature is significantly reduced. Then, temperature starts to increase due to reduction in consumption of raw materials and decrease in reactions. Finally, temperature becomes constant at 700 at equilibrium, which is minimum temperature required to prevent carbonization and carbon poisoning in the reactor. Table 9 shows changes in conversion rate considering thermal flux. Optimal thermal flux is 8000 mW/cm^2. Figure 10 shows concentration profile along the reactor.

Table 8: Thermal flux to conversion rate

	Q(mW/cm^2)	Conversion %
GHSV=5000	4000	69.6
T=800	6000	73.5
	8000	87.5

4. Discussion and Conclusion

Among industrial catalysts, nickel catalysts can control process along with compounds as well as noble metals (Pt, Rh, Ru) supported on Al2O3 and lower cost less than catalysts of noble metals.

The first section of this study modelled an ideal tubular reactor as well as kinetics and temperature conditions; the results were used in the second part of simulation. Components, coefficients and kinetic properties were extracted from references and results of experiments which were most similar to the suggested model.

This model determined conversion rate and temperature profile along the reactor. Conversion rate and temperature profile were depicted at different temperatures. Temperature calculations showed that temperature drop was directly related to reduction in conversion rate of reactor. Results of the first modelling showed that 68% conversion rate could be obtained at 5000 inlet rate, 800℃ inlet temperature, 1 atm pressure and 3.1 molar ratio. Due to endothermic nature of reaction, a considerable drop was observed in temperature; this drop reduced conversion rate along the reactor, increased catalyst poisoning and reduced yield.

In this system, the difference between inlet and outlet temperatures was approximately 400℃; this difference in temperature could considerably decrease by applying external heat to outer wall of the reactor. The second part of modelling simulated the process in a full monolith reactor in three dimensions by considering mass, heat and momentum equations. To reduce volume of calculations, simulation was done on one-eighth of the real model. Due to symmetric geometry, the assumed problem was logical and could be generalized for full reactor. Here, different scenarios are discussed. First, simulation was done under experimental conditions at 800℃, atmospheric pressure, 3.1 ratio and GHSV=5000 and the obtained values were compared with experimental values.

This process was done to validate the model. The results were relatively consistent with real values in terms of general trend and the obtained percentages. The difference in simulated and real values can be explained as follows. Due to limitation in facilities and experimental data, this modelling did not consider some components and parameters and the conditions were considered completely ideal. Number of main and adverse reactions in which experimental sample was done is more than the main and selective reaction. For example, methane decomposition reaction leading to carbonization and catalytic poisoning was not included here. Another difference is in kinetic parameters which were not consistent with experimental values of temperature.

The next problem is related to conditions such as porosity, dimensions and constituents. Another difference can be seen in coefficients and diffusion rate in porous part about which little is known. The last problem is difference in solution and computations which is inevitable. The second scenario evaluated effect of temperature on reactor yield. Here, three parameters are addressed, GHSV, inlet temperature and heat flux of wall. GHSV reduces conversion rate; by increasing temperature distribution along the reactor, however, it prevents strong temperature drop and catalyst poisoning.

Then, effect of inlet temperature is evaluated on conversion rate. Finally, effect of thermal flux is evaluated on conversion rate. The increase in flux to 8000 mW/cm^2 maximizes conversion rate and considerably reduces temperature drop.

Results of this study can be a starting point for similar simulations and implementation in laboratory and industrial scale. Here, some factors such as catalyst lifetime, which is influenced by factors such as toxicity due to presence of sulfur in feed and coke formation, are not considered. By laboratory implementation, thus, many factors discarded in simulation due to limitations such as adverse reaction and flow distribution can be considered. Here, only wall heat was applied; however, heat drop is relatively higher in the centre than walls of the reactor. To solve this problem,

central heating can be used which both improves performance and dissipates less energy due to its position in centre of the reactor.

References

1. Galluchi, F. "Experimental Study of the Methane Steam Reforming Reaction in a Dense Pd/Ag Membrane Reactor". *Journal of Industrial and Engineering Chemistry Research.*43 (4), pp. 928–933.2004.
2. Chen, J. "Mathematical modeling of monolith catalysts and reactors for gas phase reaction". *Journal of Applied Catalysis A: General*, Vol 345, pp. 1-11.2004.
3. Palma, V. "Monolithic catalysts for methane steam reforming intensification: Experimental and numerical investigations". *Journal of Fuel.* Vol 138, pp.80-90.2014.
4. Hayes, R., Fadic, A., Mmbaga, J., Najafi, A., "CFD modelling of the automotive catalytic converter". *Journal of Catalysis Today*. Vol 188, pp. 94-105. 2012.
5. Limarga, A., Shian, S., Leckie, R., Levi, C., Clarke, D., "Thermal conductivity of single- and multi-phase compositions in the ZrO2–Y2O3–Ta2O5 system". *Journal of the European Ceramic Society.* Vol 34, pp. 3085-3094. 2014.
6. Sprung, C., Arstad, B., Olsbye, U. "Methane Steam Reforming over a Ni/NiAl2O4 Model Catalyst—Kinetics". *Journal of ChemCatChem.* 6(7), pp. 1969-1982.2014.
7. Heck, R., Gulati, S., Farrauto, R., "The application of monoliths for gas phase catalytic reactions" *Chemical Engineering Journal.* Vol 82, pp. 149-156.2001.